芸術科学会論文誌 Vol. 13 No. 1 pp. 11 – 20

Micro-Geometric Skin Simulation for Face Impression Analysis

Fumie Banba[1)] **Takayuki Itoh**[1)]
Mami Inomata[1)] **Mihayu Kurokawa**[1)]
Naruhito Toyoda[2)] **Hitomi Otaka**[2)] **Hiromi Sasamoto**[2)]

1) Ochanomizu University 2) Shiseido Co. Ltd.,
{mie, mami, mihayu, itot} (at) itolab.is.ocha.ac.jp

Abstract

Condition of skin is an important factor for the impression of faces. Well-cared skins give shiny and beautiful impression, while dry and rough skins loss the gloss and therefore they are less attractive. These differences often attribute to the difference of their micro-geometry. Such micro-geometry of human skins consists of furrows forming a mesh, ridges surrounded by the furrows, and pores. This paper presents a technique for micro-geometry simulation of human skins. The technique first generates pores forming a pattern of a well-aligned triangular grid. It then divides the skin region by applying the Delaunay triangulation algorithm to connect the pores. It treats the triangles as ridges, and the edges as furrows. Finally, the technique divides the pattern into a finer triangular mesh, so that it can finely represent 3D geometry of pores, ridges, and furrows. This paper also presents a technique for image recognition of micro-geometry parameters of real human skins. It features two-steps of template-matching-like algorithms: the former one acquires sizes of pores, and the latter one acquires widths and directionality of furrows. These results are consumed by the skin simulation technique as input parameters of the micro-geometry.

1 Introduction

Many people are interested in keeping their skins fine, and therefore skin maintenance is an important technology for many people. Well-cared skins give shiny and beautiful impression. Dry and rough skins loss the gloss and therefore they are less attractive. Condition of skin is therefore an important factor for the impression of faces.

Our project is focusing on impression analysis of various conditions of skins. We have already had several experiments which showed images of various conditions of face skins to subjects, and aggregated their answers on impressions of the skins. These experiments have a difficulty: it is quite hard to obtain real photographs of various conditions of skins. Conditions of skins are related to both geometric and optical properties, and the combination of such properties is enormous. In addition, we often would like to control external conditions such as lighting and viewing settings. It is not practical to gather all the possible combinations of the conditions as real photographs. Therefore, we are also using images of faces generated by computer graphics techniques for the impression analysis, as an alternative solution. Computer graphics is very useful for this purpose because it can flexibly control geometric, optical, and viewing properties. Our study [1] proved that impression analysis using computer graphics is sufficiently feasible, because the result is quite similar and correlative with the results of impression analysis using real photographs.

Meanwhile, it is well-known that micro-geometry of skins (including pores, ridges, and furrows) greatly affects to their conditions. It is therefore very important for cosmetics and beauty technology development to analyze the relationship and correlation between micro-geometry of skins and their impressions. Based on this discussion, we are extending our study to analyze the relationship and correlation between micro-geometry of skins and their impressions. This paper presents a skin simulation technique which generates micro-geometry of face skins as a set of very fine triangular polygons. The technique first generates pores forming a pattern of a well-aligned triangular grid on a 2D skin region. It then generates triangular ridges by dividing the skin region by connecting the centers of pores applying the Delaunay triangulation algorithm. The technique divides the ridges and pores into a finer triangular mesh, while calculating the displacements of the vertices of the mesh. Consequently, it can finely represent 3D geometry of pores, ridges, and furrows. Finally, the triangular mesh is mapped onto 3D face geometry and finely rendered.

The above micro-geometric skin simulation technique requires many parameters for pores, ridges, and furrows. We experimentally found that it is not always feasible to easily and adequately control the micro-geometry with smaller number of parameters; we concluded that it may be useful if we can acquire some of the parameters from real photographs. This paper also presents a technique for micro-geometry parameter acquisition from photographs of real skins. The technique features two-steps of template-matching-like algorithms: the former one acquires the statistics of sizes of pores, and the latter one acquires the statistics of widths and directionality of furrows. These results are formed as histograms, and consumed by the micro-geometry generation technique as input parameters.

This paper presents several results on micro-geometry generation and parameter acquisition.

2 Related Work

2.1 Micro-geometry of skins

Micro-geometry of skins is generally formed by holes of hairs (called *pores*), channels connecting the pores and constructing meshes (called *furrows*), and bumps enclosed by the furrows (called *ridges*). Figure 1 illustrates the micro-geometry and explains the above terms. It is well-known that micro-geometry of well-cared face skins usually form triangular patterns. Especially, skins around cheeks form relatively regular triangular patterns. In this paper we focus on the simulation of such triangular patterns, because impression analysis around cheeks is especially important for cosmetics development.

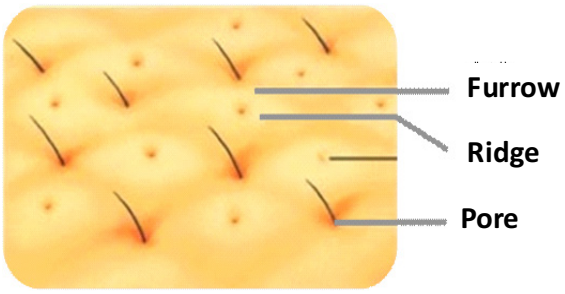

Figure 1: Definition of terms: furrow, ridge, and pore.

2.2 Parameter acquisition and impression analysis for skins

Cosmetics researchers have actively presented skin analysis technologies. Sasaki et al., [2] presented a technique to calculate fractal dimensions and entropy from the bumpyness of skin surfaces measured by radiating laser beams to the replicas of the skins. The study

demonstrates the fractal dimensions and entropy correlate with subjective impressions of the skins. Nishimura et al., [3] presented a study to explore the correlation between their impressions and measured properties including moisture contents, geometric features, and optical properties.

These techniques seem quite expensive since they need special measurement equipments. On the contrary, we focus on parameter acquisition from ordinary photographs because it does not require special measurement equipments and therefore it will be easier to be common.

2.3 Computer graphics for representation of skins

Representation of human is a very important topic in computer graphics. Modeling and rendering of human skin is also an important problem for the representation of human, and actually many techniques have been presented.

This section introduces techniques on modeling of human skins, since this paper focuses on modeling of micro-geometry of skins. Bando et al., [4] presented a technique to generate wrinkles along given vector fields. Wu et al. [5] presented a technique for representation of aging of skins. These techniques did not focus on micro-geometry such as pores and furrows. Halo et al. [6] presented a technique to reproduce micro-geometry of skins. Ghost et al. [7] presented a technique for acquisition and rendering of micro-geometry of face skins with multi-view photographs of high-resolution cameras. These technique requires special equipments for measuring micro-geometry of real human skins as input datasets.

3 Overview of the Presented Study

This section presents an overview of our study, consisting of the following technical components. Figure 2 illustrates the processing flow of the presented study.

Parameter acquisition: This component detects pores and furrows from real photographs of micro-geometry of skins, and determines their parameters.

Micro-geometry generation: This component generates a pattern of pores, ridges, and furrows, and then polygonizes the geometry. It consumes several parameters from the acquisition results while other parameters can be manually adjusted.

Mapping to face geometry: This component maps the micro-geometry onto the face geometry, supposing that texture parameter coordinates are assigned to the face geometry. Also, this components synthesizes realistic images of the face skins.

Impression analysis: This component visualizes impression analysis results by applying a multi-dimensional data visualization technique. We asked subjects to answer the impression of images of skins generated by the above processes, and applied the statistics of the answers to this component.

This paper mainly proposes the former three components. Section 4 presents components of micro-geometry generation and face geometry mapping, and Section 5 presents a component of parameter acquisition.

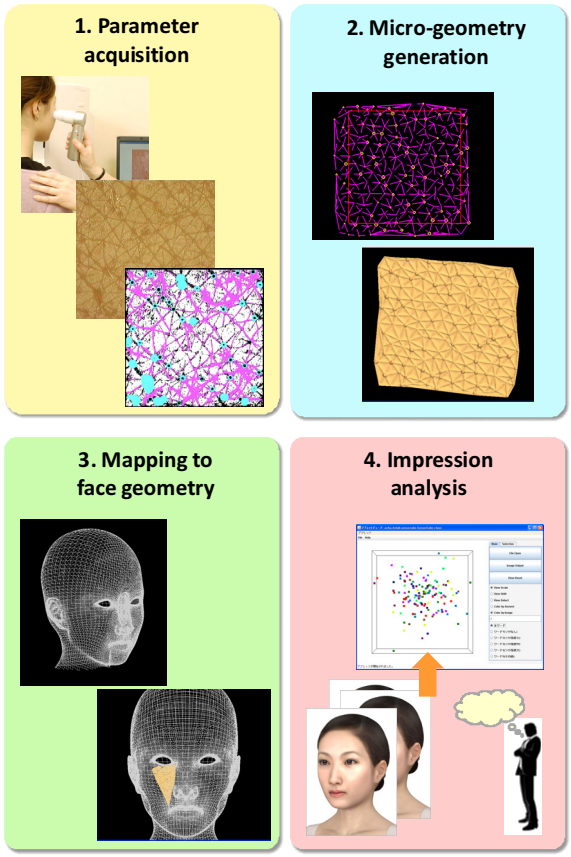

Figure 2: Overview of the presented study.

4 Image Recognition for Parameter Acquisition

This section presents a technique for acquisition of micro-geometry parameter by an image recognition technique for real photographs of skins. The section firstly describes the algorithm to detect pores and furrows from real photographs of skins. It then describes parameter construction and micro-geometry generation based on the pore and furrow detection results.

4.1 Detection of pores and furrows

Our current implementation for pore and furrow detection simply binalizes the real photographs, and detects circular or thin black regions. Our experiments demonstrate that this straightforward implementation can adequately detect pores and furrows from our own photographs of skins. The detailed processing flow is described as follows.

4.1.1 Binalization

Our implementation firstly applies binalization to the input image. It converts pixels into white if the sums of their RGB values exceed the pre-defined threshold. Otherwise, it converts them into black. The current implementation manually specifies the threshold experimentally and subjectively. We would like to develop a discriminate analysis scheme to adequately specify the threshold.

4.1.2 Pore detection

The technique then detects circular black regions from the binalized images. It applies a template-matching-like algorithm to scan the images by using various sizes of circular templates. Figure 3(Left) is an illustration of the algorithm for the pore detection. The detailed processing flow is as follows:

1. Prepare a circular template whose diameter is $2r$. Scan the circular template all over, and apply the following procedures at the each of the scanned positions.
   (a) Count the total number of black pixels inside the circular template.
   (b) If the number of the black pixels exceeds a pre-defined threshold. treat the region where the template locates as a pore. In this case, record the radius and center of the template, and convert the counted black pixels into while so that the technique never detect the pore inside the region again.
2. Let the diameter of the new template $2r = 2r - 1$. Return to 1.
3. Repeat 1. and 2. until the diameter becomes below a pre-defined threshold.

4.1.3 Furrow detection

The technique also detects thin black regions from the binalized images. It applies a template-matching-like algorithm to scan the images by using various directions of thin templates. Figure 3(Right) is an illustration of the algorithm for the furrow detection. The detailed processing flow is as follows:

1. Prepare a thin template. Scan the template all over, and apply the following procedures at the each of the scanned positions.
   (a) Count the total number of black pixels inside the thin template.
   (b) If the number of the black pixels is below a pre-defined threshold, treat that this region is not a furrow, and return to 1.
   (c) Otherwise, treat this region as a furrow. In this case, slide the template and similarly count the number of black pixel inside the thin template. Repeat this procedure until the number becomes below the pre-defined threshold, and treat the number of the repetition as a width of the furrow. Record the center and direction of the template, width of the furrow, as the parameters of the furrow.
2. Repeat the above process with various directions of the thin templates. Our current implementation prepares 16 directions.

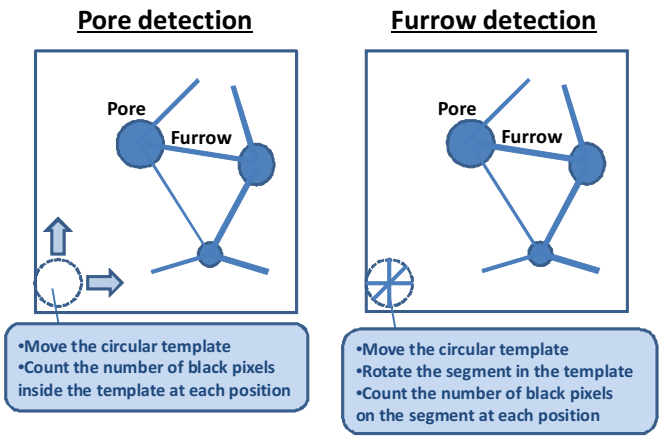

Figure 3: (Left) Pore detection. (Right) Furrow detection.

4.2 Parameters of pores and furrows for micro-geometry simulation

After detecting pores and furrows, the technique forms parameters of pores and furrows as histograms. They are consumed by the micro-geometry simulation

4.2.1 Parameter of pores

The technique aggregates the radii of pores, and forms their histogram as a parameter of micro-geometry simulation. While generating pores as described in Section 5.2, the micro-geometry simulation technique assigns radii to the pores, where the possibility of the radii is proportional to their frequency in the histogram. This mechanism adequately adjusts the distribution of radii of pores in the micro-geometry simulation while avoiding manual operations for parameter setting. It simultaneously adjusts the distribution of depths of pores, under the assumption that their depths are proportional to the radii.

4.2.2 Parameter of furrows

The technique aggregates the width and directionality of furrows, and form their histograms as parameters of micro-geometry simulation, as well as radii of pores. While generating furrows as described in Section 5.2, the micro-geometry simulation technique assigns widths to the furrows, where the possibility of the widths is proportional to their frequency in the histogram. Also, the technique assigns depths to the furrows, where deeper depths are assigned if their direction is more frequent. Consequently, frequent directions of furrows look more visible in the micro-geometry simulation results. This mechanism adequately adjusts the distribution of width and directionality of furrows in the micro-geometry simulation while avoiding manual operations for parameter setting.

5 Micro-Geometric Skin Simulation

This section presents a technique for 3D modeling of skin micro-structure which freely generates various skins by controlling the parameters described in this section. The technique firstly generates patterns of pores, ridges, and furrows, by connecting evenly generated pores applying Delaunay triangular meshing. It then tessellates the patterns into fine triangular polygons applying Delaunay triangular meshing again. Finally, it maps the micro-geometry onto the face geometry. This section firstly introduces our observation of real skin photographs to specify the input parameters for the micro-geometry generation, and then describes the presented technique.

5.1 Observation for parameter specification

We captured micro-geometry of real human skins to discuss and design the modeling technique. We subjectively observed skins in the following three conditions, shown in Figure 11, which are especially important for cosmetics analysis:

[**1: Well-cared skin**] Furrows are continuous. Ridges are regularly aligned, equally-sized, and roundly.

[**2: Pore-expanded skin**] Pores are not only large but also deep.

[**3: Dry skin**] Ridges are flat but regularly aligned. However, furrows are so depthless that patterns are unclear.

Based on the above observation, we concluded that the following parameters should be controllable while representing micro-geometry of skins:

[**Pore:**] Radius, depth, and randomness of positions. Here, radius and depth can be automatically adjusted with the parameters acquired from real images, as described in Section 4.2.1. Randomness of positions are to be adjusted by users.

[**Ridge:**] heights, and randomness of heights. These values are to be adjusted by users.

[**Furrow:**] depths, widths, and directional dependency. These values can be automatically adjusted with the parameters acquired from real images, as described in Section 4.2.2.

5.2 Pattern generation

Figure 4(Upper) shows an illustration of processing flow of the pattern generation, including generation of pores, ridges, and furrows.

This step first prepares a well-aligned triangular grid inside a given region, and generates a set of pores on the vertices of the grid. Here, it controls radii and depths of the pores based on the predefined parameters. Perturbation is also applied to radii and positions of pores by adding random values.

The technique then divides the skin region by connecting the centers of pores. It applies a progressive Delaunay triangulation algorithm [8] to generate triangular subregions. The technique treats the triangles as ridges, and the edges as furrows, and controls their shapes based on the parameters. Here, moderately randomized heights are assigned to each of the ridges, while moderately randomized depths and widths are assigned to each of the furrows. Also, depths of furrows are controlled based on directional dependency: the technique assigns larger depths to particular directions of furrows, and smaller depths to others, when stronger dependency is supposed.

5.3 Polygon generation

The technique then divides the pattern into a finer triangular mesh, so that it can represent smoothly curved 3D geometry of pores, ridges, and furrows.

The technique first generates vertices of the triangular mesh. It generates vertices inside pores on their centers

and concentric circles. It evenly generates vertices on the furrows. It also evenly generates vertices inside the ridges, and assigns heights so that they form a smoothly curved surface. Figure 4(Lower) shows an illustration of the vertex generation, inside the pores, on the furrows, and inside the ridges.

Finally, the technique generates a finer triangular mesh by applying the Delaunay triangular mesh to connect the vertices.

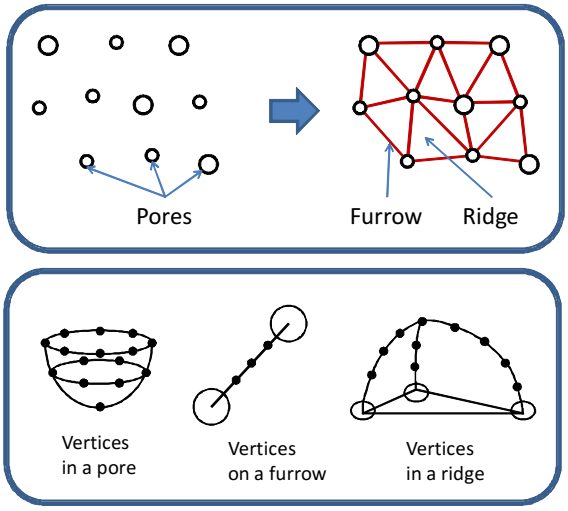

Figure 4: (Upper) Processing flow of the pattern generation. (Lower) Processing Flow of the polygon generation.

5.4 Mapping to face geometry

The technique then maps the micro-geometry of the skin onto the face geometry. Figure 5 illustrates this process. Here, it supposes that the face geometry is given as a set of triangles, and their vertices have coordinate values in a 3D world (x, y, z) and in a 2D texture world (u, v). Also, it supposes that the micro-structure is generated as bumps on a XY-plane, and the Z coordinate values of their vertices correspond to the displacements of the XY-plane.

1. Let texture coordinate values of a triangle of the face geometry as

   $A_1(u_1, v_1)$, $A_2(u_2, v_2)$, and $A_3(u_3, v_3)$.
   Given a vertex of the micro-geometry $B(u_B, v_B)$, the technique specifies the triangle of the face geometry which encloses B.

2. Connect B and each of A_1, A_2, and A_3 to form three triangles. Let the areas of the triangles as follows.

$$s_1 = (area\_of\_BA_2A_3)$$
$$s_2 = (area\_of\_BA_3A_1)$$
$$s_3 = (area\_of\_BA_1A_2)$$

3. Let the coordinate values of the three vertices of the specified triangle as $A_1(x_1, y_1, z_1)$, $A_2(x_2, y_2, z_2)$, and $A_3(x_3, y_3, z_3)$, in the 3D world. Calculate the coordinate values of $B(x'_B, y'_B, z'_B)$ by the following equations:

$$x'_B = s_1x_1 + s_2x_2 + s_3x_3$$
$$y'_B = s_1y_1 + s_2y_2 + s_3y_3$$
$$z'_B = s_1z_1 + s_2z_2 + s_3z_3$$

4. Calculate the normal vector of $B(a_B, b_B, c_B)$ by similarly interpolating the normal vectors of A_1, A_2, and A_3.

5. Calculate the final coordinate values $B(x'_B, y'_B, z'_B)$, where r is the displacement of B on the XY-plane.

$$x'_B = x'_B + a_Br$$
$$y'_B = y'_B + b_Br$$
$$z'_B = z'_B + c_Br$$

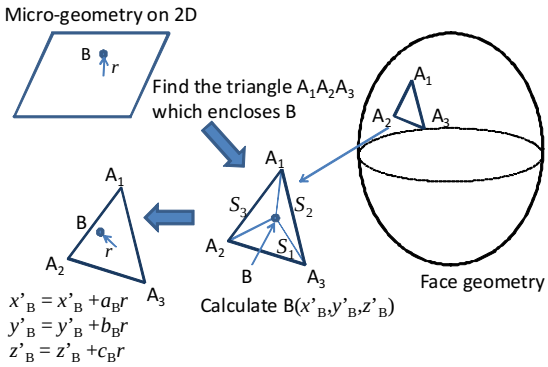

Figure 5: Mapping micro-geometry onto the face geometry.

Our current implementation divides the face geometry into several parts as shown in Figure 6(Left) based on the knowledge of cosmetics engineering, then independently generate micro-geometry for each of the parts, and finally maps all the micro-geometry as shown in Figure 6(Right). It is well-known that each part has different properties of the micro-geometry, and therefore it is preferable that our implementation can independently adjust parameters for each part.

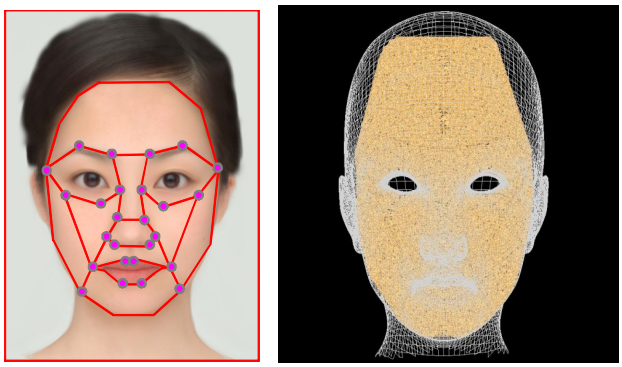

Figure 6: Mapping to the face geometry. (Left) Parts of a face. (Center) (Right) Example of micro-geometry mapping of the all parts.

Data size is another issue. The polygon dataset shown in Figure 6 contains 1431594 triangles and 727609 vertices; it may be difficult to realize high frame rate on low-cost platforms. However, it is not a serious problem for the purpose of our project. Still images are commonly used for impression analysis in cosmetics industry rather than interactive applications, and therefore high frame rate is not important for our purpose. Meanwhile, high resolution geometric modeling is more important for our purpose, because we may require high resolution images for printing the images on the high quality papers rather than looking on the digital displays. Also, we often use partially zoomed images of faces for impression analysis; in this case number of rendered polygons is much less than rendering whole the face. For example, number of triangles and vertices of a cheek shown in Figure 10(Left) are 74716 and 38169 respectively.

6 Example

This section shows examples of micro-geometry simulation and parameter acquisition. Here, it is well-known that geometric patterns and parameters vary based on the parts of the face. This section shows examples real photographs and simulations of skins on the cheek of faces.

6.1 Examples of parameter acquisition

Figure 7 shows examples of real photographs and detection results. Sky blue parts in the right figures denote detected pores, while pink parts denote detected furrows. This result demonstrates that the presented parameter acquisition technique well detects most of pores and furrows. However, it may happen that thick furrows are detected as pores. We need to adjust hard-coded parameters such as threshold of binalization step, and maximum/minimum sizes of templates for pores and furrows, to reduce such detection errors.

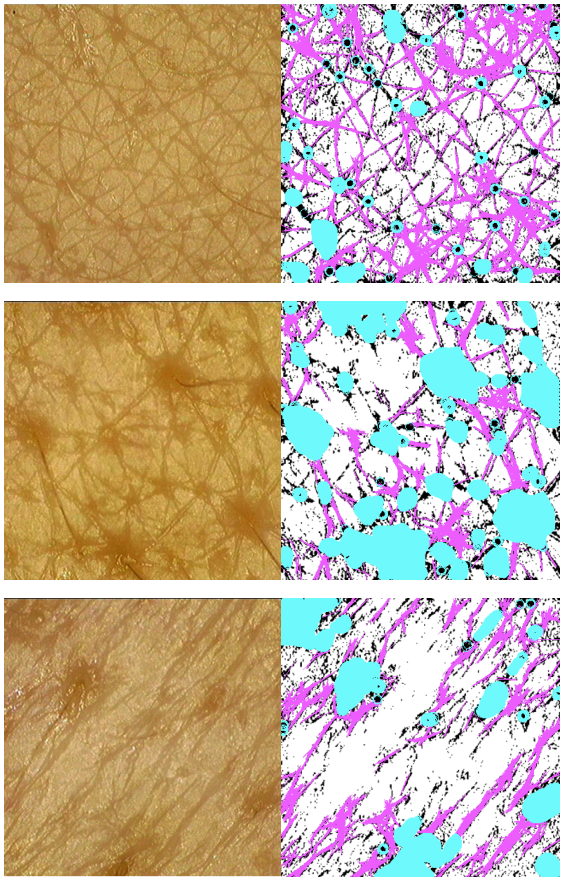

Figure 7: Real photograph and detected pores / furrows. (Upper) Well-cared skin. (Center) Pore-expanded skin. (Lower) Dry skin.

Figure 8 shows an example of pattern and polygon generation result consuming a histogram of pore radii captured from a real photograph.

Figure 9 shows an example of histograms of directions of furrows captured from three real photographs. The histogram denotes the numbers of detected furrows using each of 16 directions of templates. Here, the histograms from well-cared and pore-expanded skins have multiple peaks, while the histogram from a dry skin have a single peak. Actually, it is well-known that furrows of dry skins often form particular directions. This result demonstrates that detection of furrow direction is important to determine the conditions of skins.

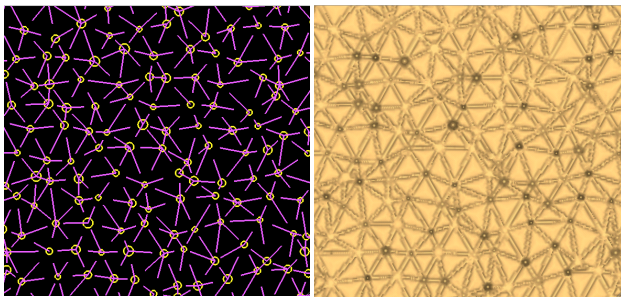

Figure 8: Pattern and polygon generation result consuming a histogram of pore radii captured from a real photograph.

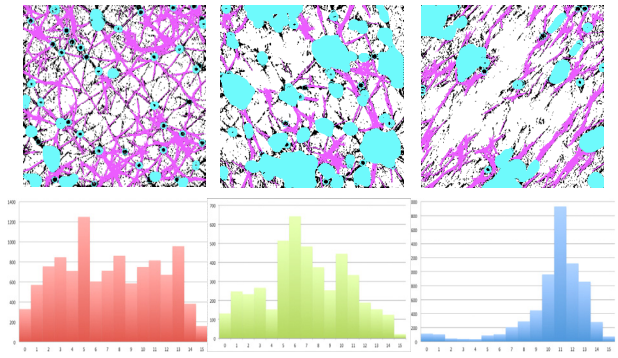

Figure 9: Histogram of directions of furrows. (Left) Well-cared skin. (Center) Pore-expanded skin. (Right) Dry skin.

6.2 Examples of micro-geometry simulation

Figure 10 shows examples of skin simulation results mapped onto the geometry of a cheek. We rendered these examples by blending the intensity of the micro-geometry with texture-mapped images of real skins.

Figure 11 (Upper) shows an example of real photograph and simulation result of a well-cared skin. It forms a quite regular triangular patterns of ridges and furrows. Sizes of pores moderately vary. Figure 11 (Center) shows an example of real photograph and simulation result of a pore-expanded skin. Sizes of pores are relatively larger, while it also forms a quite regular triangular patterns. Figure 11 (Lower) shows an example of real photograph and simulation result of a dry skin. Ridges and furrows are relatively flat. We showed the results to experts of skin care technologies, and received good comments that these figures well express the conditions of skins.

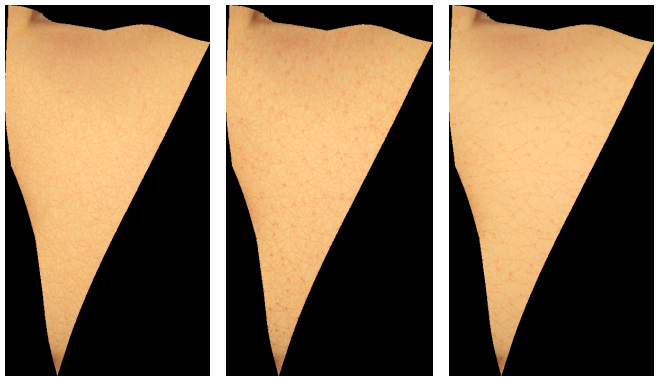

Figure 10: Skin mapped onto the cheek geometry. (Left) Well-cared skin. (Center) Pore-expanded skin. (Right) Dry skin.

7 Conclusion

This paper presented our study on micro-geometric skin modeling. The technique represents shapes of pores, ridges, and furrows as very fine triangular polygons, and maps them onto the face geometry. The paper also presented our study on micro-geometry parameter acquisition from real photographs. The technique applies a template-matching-like algorithm to detect pores and furrows from the photographs, and determines the micro-geometry parameters as input setting of skin modeling. This paper presented several examples on skin modeling and parameter acquisition, and brief results of their impression analysis.

Potential future issues of this study include the following.

[**Fast and realistic rendering:**] This paper did not mention rendering issues, because we needed to use our own unpublished rendering framework in this project. Also, our preliminary study [1] has already demonstrated that the quality of our current rendering results is sufficient for the face impression analysis. From these results, we have not well discussed regarding the improvement of rendering speed and quality. However, of course it is important to discuss rendering issues in this research field. We would like to consider optical properties of skins such as anisotropic specular and sub-surface scattering components for more realistic image generation. Also, we would like to consider GPU based and polygonless implementation for more interactive purposes. Another research issue is that our current implementation may cause gaps of the geometry on the border of the parts, as shown in Figure 12. Though we do not think this problem seriously affect to the impression analysis results, we would like to solve it by generating pores and

vertices on the border first, and sharing them by two parts adjacent to the border.
[**Enhancement of parameter acquisition:**] Our current implementation of template-matching-like algorithm have sufficient results for our explements; however, it needs manual configuration of parameters such as threshold of binalization and sizes of templates. We would like to develop automatic parameter configuration techniques, when we specify the photographing equipments on this project.
[**More impression analysis:**] We know that the impression of skins correlates with various components such as age and feeling of subjects, optical setting, and shapes of faces, in addition to micro-geometry parameters. This paper just presented a brief result with varying micro-geometry parameters. We would like to continue impression analysis with more variety of optical and geometric settings, and more subjects.

References

[1] M. Inomata, T. Itoh, N. Toyoda, Impression evaluation and visualization of texture of skin, *The 3rd Forum on Data Engineering and Information Management*, E7-2, 2011. (in Japanese)

[2] T. Sasaki, M. Nakagawa, Quantitative Evaluation Method of Skin Surface with Fractal Dimensions and Entropy Measure, *IEICE Technical Report, Nonlinear Problems*, 108(442), pp. 49-54, 2009. (in Japanese)

[3] 西村博睦，高須賀豊，山本めぐみ，”肌ツヤの光学特性とみずみずしく見えるメークアップファンデーションの開発研究，”日本化粧品技術者会誌, Vol. 40, No. 2, pp. 88-94, 2006. (in Japanese, no English title)

[4] Y. Bando, T. Nishita, Human Skin Simulation by Generating Wrinkles along Vector Fields, *Visual Computing / Graphics and CAD joint symposium*, 2001. (in Japanese)

[5] Y. Wu, P. Kalra, L. Moccozet, N.-M. Thalmann, Simulating Wrinkles and Skin Aging, *The Visual Computer*, Vol. 15, No. 4, pp. 183–198, 1999.

[6] A. Haro, B. Guenter, I. Essa, Real-time Photorealistic Physically Based Rendering of Fine Scale Human Skin Structure, *12th Eurographics Workshop on Rendering Techniques*, 53-62, 2001.

[7] A. Ghosh, G. Fyffe, B. Tunwattanapong, J. Busch, X. Yu, P. Debevec, Multiview Face Capture using Polarized Spherical Gradient Illumination, *ACM Transactions on Graphics (Proceedings of SIGGRAPH ASIA)*, Vol. 30, No. 6, p. 129, 2011.

[8] S. W. Sloan, A Fast Algorithm for Constructing Delaunay Triangulations in the Plane, *Advances in Engineering Software*, Vol. 9, No. 1, pp. 34-55, 1987.

番場 文枝

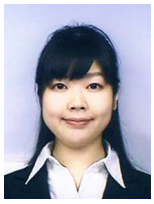

2013 年お茶の水女子大学理学部情報科学科卒業．現在お茶の水女子大学大学院人間文化創成化学研究科理学専攻博士前期課程在学中.

伊藤 貴之

1990 年早稲田大学理工学部電子通信学科卒業．1992 年早稲田大学大学院理工学研究科電気工学専攻修士課程修了．同年日本アイ・ビー・エム (株) 入社．1997 年博士 (工学)．2000 年米国カーネギーメロン大学客員研究員．2003 年から 2005 年まで京都大学大学院情報学研究科 COE 研究員 (客員助教授相当)．2005 年日本アイ・ビー・エム (株) 退職，お茶の水女子大学理学部情報科学科助教授．2011 年同大学教授，同大学シミュレーション科学教育研究センター長．ACM, IEEE Computer Society, 情報処理学会，芸術科学会，画像電子学会，可視化情報学会，他会員.

猪股 真美

2011 年お茶の水女子大学理学部情報科学科卒業．2013 年お茶の水女子大学大学院人間文化創成化学研究科理学専攻博士前期課程修了.

黒川 海映

2010 年お茶の水女子大学理学部情報科学科卒業．2012 年お茶の水女子大学大学院人間文化創成化学研究科理学専攻博士前期課程修了.

豊田 成人

1993 年法政大学大学院システム工学研究科修士課程修了，同年（株）資生堂入社．美容情報開発・美容機器開発を経て 2009 年よりコンピュータグラフィックスを用いた化粧の印象や嗜好性研究に従事．

大高 瞳

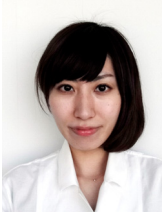

2009 年慶應義塾大学大学院理工学研究科修士課程修了，同年（株）資生堂入社．スキンケア製品開発業務を経て 2011 年より触感評価法開発，化粧質感の嗜好性研究に従事．

笹本 裕美

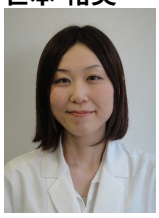

2007 年筑波大学大学院生命環境科学科修士課程修了，同年（株）資生堂入社．メーキャップ製品開発業務を経て 2008 年より使用感評価法開発，化粧質感の嗜好性研究に従事．

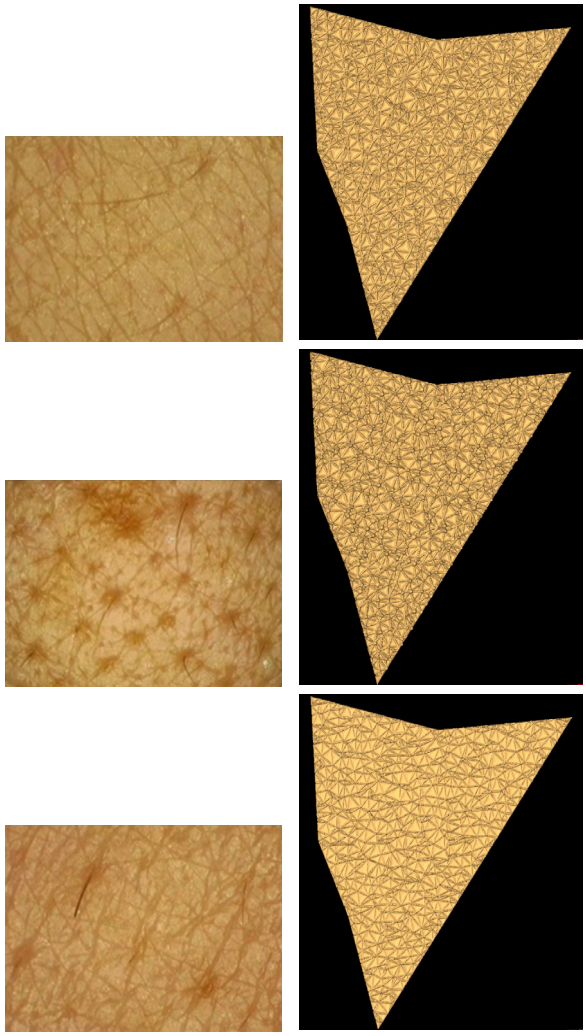

Figure 11: (Upper) Real photograph and simulation result of a well-cared skin. (Center) Real photograph and simulation result of a pore-expanded skin. (Lower) Real photograph and simulation result of a dry skin.

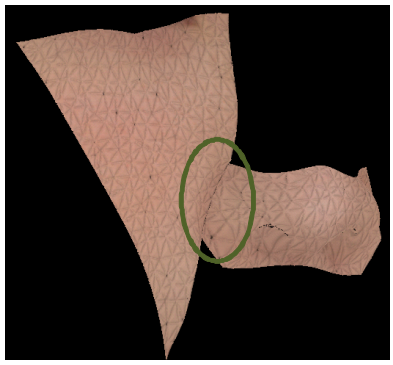

Figure 12: A gap of meshes on the border of two parts.